JOURNAL OF SEMICONDUCTOR TECHNOLOGY AND SCIENCE, VOL.17, NO.1, FEBRUARY, 2017 ISSN(Print) 1598-1657
https://doi.org/10.5573/JSTS.2017.17.1.029 ISSN(Online) 2233-4866

A CMOS-based Temperature Sensor with Subthreshold Operation for Low-voltage and Low-power On-chip Thermal Monitoring

Jun-Seok Na, Woosul Shin, Bong-Choon Kwak, Seong-Kwan Hong, and Oh-Kyong Kwon

Abstract—**A CMOS-based temperature sensor is proposed for low-voltage and low-power on-chip thermal monitoring applications. The proposed temperature sensor converts a proportional to absolute temperature (PTAT) current to a PTAT frequency using an integrator and hysteresis comparator. In addition, it operates in the subthreshold region, allowing reduced power consumption. The proposed temperature sensor was fabricated in a standard 90 nm CMOS technology. Measurement results of the proposed temperature sensor show a temperature error of between −0.81 and +0.94°C in the temperature range of 0 to 70°C after one-point calibration at 30°C, with a temperature coefficient of 218 Hz/°C. Moreover, the measured energy of the proposed temperature sensor is 36 pJ per conversion, the lowest compared to prior works.**

Index Terms—**Temperature sensor, low-voltage low-power, subthreshold current, PTAT, temperature-to-frequency converter**

Manuscript received Oct. 17, 2016; accepted Jan. 15, 2017
A part of this work was presented at 23rd Korean Conference on Semiconductors, Jeongseon, Korea, Feb. 2016.
The authors are with the Department of Electronics Engineering, Hanyang University, Seoul 133-791, Korea
E-mail : skysholo@hanyang.ac.kr; woosulshin@hanyang.ac.kr; dikari@hanyang.ac.kr; seongkhong@hanyang.ac.kr; okwon@hanyang.ac.kr

I. INTRODUCTION

In various applications such as wireless sensor networks, radio frequency identification (RFID), automotive systems, microprocessors, DRAM, and energy harvesting systems, temperature sensors are needed to monitor the thermal profile of the integrated chip because the temperature affects the performance such as speed, power, and reliability. For on-chip thermal monitoring, the temperature sensor needs to have characteristics such as low supply voltage, low power consumption, and moderate temperature accuracy [1, 2].

Several researches on temperature sensors have been carried out to monitor the thermal profiles of chips [2-11]. In general, a bipolar junction transistor (BJT) or MOSFET fabricated in CMOS process is used to sense the temperature so that the voltage/current and time-domains can be represented as a function of temperature. The temperature sensor, which produces a voltage/current according to the temperature, uses the base–emitter voltage and saturation current of the BJT [3], the threshold voltage and mobility of the MOSFET [4], or the gate–source voltage of the MOSFET in the subthreshold region [5]. The BJT-based temperature sensor has a high temperature accuracy, whereas the MOSFET-based temperature sensor has a moderate temperature accuracy. However, both temperature sensors have high power consumption because they require the use of analog-to-digital converters to convert the voltage/current. For low-power on-chip temperature monitoring, a time-domain temperature sensor has been introduced to generate a frequency, a delay, or a duty

cycle of a pulse according to the temperature [2, 6-11].

In this paper, we propose a temperature sensor for low supply voltage and low power consumption using MOSFETs that operate in the subthreshold region. The proposed on-chip temperature sensor, which is designed for monitoring the thermal profile of the organic light-emitting diode (OLED) on silicon microdisplays, converts a current to a frequency according to the temperature. To improve the temperature accuracy, the proposed temperature sensor employs an error amplifier and an integrator to minimize the difference of proportional to absolute temperature (PTAT) currents and to maintain the constant PTAT current during the integration operation, respectively. Since the properties of the OLED severely vary at high temperature due to glass transition [12], the proposed temperature sensor is designed to operate in the temperature range of 0 to 70°C.

Section II explains the operation principle and architecture of the proposed temperature sensor. Section III describes the circuit implementation of the proposed temperature sensor, which consists of a PTAT current generator, a reference voltage generator, and a current-to-frequency converter. In Section IV, the measurement results are analyzed and compared with those of prior works. Finally, conclusions are given in Section V.

II. Operation Principle of The Proposed Temperature Sensor

Fig. 1 shows a block diagram of the proposed temperature sensor which consists of a PTAT current generator, a reference voltage generator, an integrator, and a hysteresis comparator. The proposed temperature sensor produces a PTAT frequency (f_{PTAT}) according to the temperature. The PTAT current generator generates a PTAT current (I_{PTAT}) using a reference frequency (f_{REF}). The reference voltage generator provides a reference voltage (V_{REF}) to the integrator and hysteresis comparator. A combination of the integrator and hysteresis comparator is used as a current-to-frequency converter. The integrator generates a comparison voltage (V_{CMP}) by integrating I_{PTAT} based on V_{REF} and the hysteresis comparator generates f_{PTAT} by comparing V_{CMP} with V_{REF}. Then, f_{PTAT} is fed to the integrator to reset V_{REF}. Thus, the current-to-frequency converter converts I_{PTAT} to f_{PTAT}.

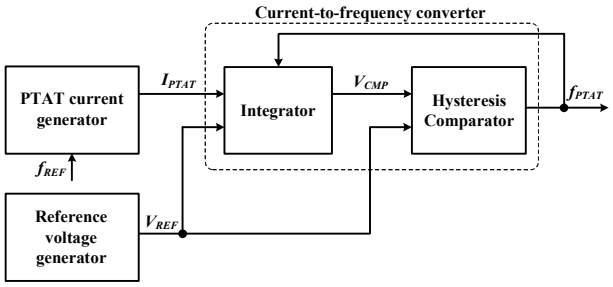

Fig. 1. Block diagram of the proposed temperature sensor.

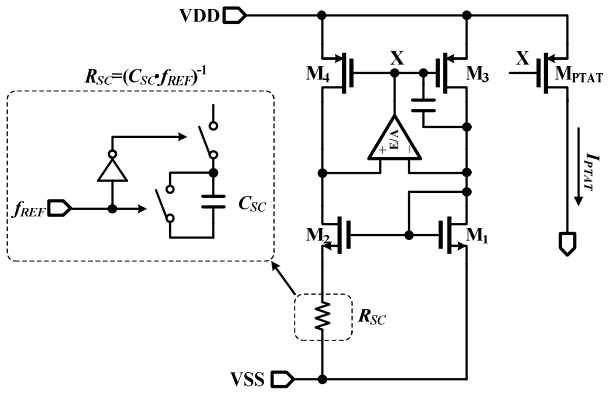

Fig. 2. Schematic of the PTAT current generator.

III. Circuit Implementation

1. PTAT Current Generator

Fig. 2 shows a schematic of the PTAT current generator, which is used as the temperature sensor core. All MOSFETs in the PTAT current generator operate in the subthreshold region for low power consumption. In the low supply voltage operation, an error amplifier is used to bias node X so that the difference between the drain voltages of M_3 and M_4 can be minimized. A switched-capacitor resistor, consisting of a capacitor C_{SC} and two switches driven by a two-phase non-overlapping clock, is used to replace the physical resistor for highly accurate and tunable analog circuits [13]; the equivalent resistance R_{SC} of this resistor is equal to $(C_{SC}\cdot f_{REF})^{-1}$.

I_{PTAT} is generated as follows. The voltage between the gate and source of M_1 ($V_{GS,M1}$) is equal to the sum of the voltage between the gate and source of M_2 ($V_{GS,M2}$) and the voltage drop across R_{SC}. Then, $V_{GS,M1}$ can be expressed as

$$V_{GS,M1} = V_{GS,M2} + I_{SC}R_{SC}, \quad (1)$$

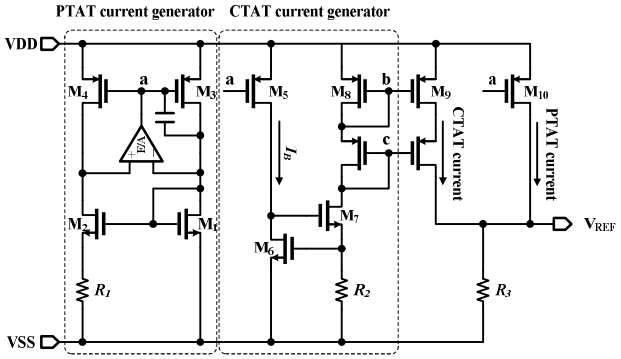

Fig. 3. Schematic of the reference voltage generator.

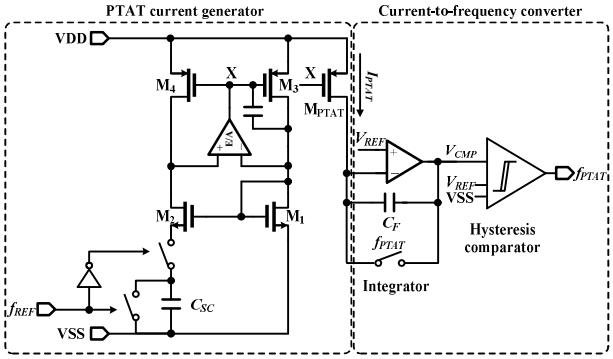

Fig. 4. Schematic of the current-to-frequency converter with PTAT current generator.

where I_{SC} is the current flowing through R_{SC}. When the voltage between the drain and source of the MOSFET is much greater than the thermal voltage (kT/q), the subthreshold current of MOSFETs can be expressed as [14]

$$I_{D,sub} = \mu_0 C_{OX} K (\eta - 1)\left(\frac{kT}{q}\right)^2 \exp\left[\frac{q(V_{GS} - V_{th,})}{\eta kT}\right], \quad (2)$$

where μ_0, C_{OX}, K, V_{th}, k, T, q, and η are respectively the zero bias mobility, the gate oxide capacitance, the aspect ratio of the transistor, the threshold voltage of the transistor, the Boltzmann's constant, the temperature, the electron charge, and the subthreshold slope factor. Because the currents flowing through M_1 and M_2 are equal, from Eqs. (1, 2), I_{PTAT} of M_{PTAT} mirrored by M_3 can be expressed as

$$I_{PTAT} = f_{REF} \cdot C_{SC} \cdot \frac{K_{MPTAT}}{K_{M3}} \cdot \frac{\eta kT \ln(K_{M2}/K_{M1})}{q}. \quad (3)$$

Therefore, I_{PTAT} is linearly proportional to temperature.

2. Reference Voltage Generator

Fig. 3 shows a schematic of the reference voltage generator, in which all MOSFETs operate in the subthreshold region. The reference voltage generator includes a PTAT current generator and a complementary to absolute temperature (CTAT) current generator. The PTAT current generator in the reference voltage generator has a structure similar to that used as the temperature sensor core as shown in Fig. 2, except that the switched-capacitor resistor is replaced by a physical resistor. Because both PTAT current generators operate in the same way, the drain current of M_3 (I_{M3}), which is mirrored to the drain current of M_5 (I_B), can be derived from Eq. (3) as

$$I_{M3} = \frac{\eta kT \ln(K_{M2}/K_{M1})}{qR_1}. \quad (4)$$

The voltage between the gate and source of M_6 ($V_{GS,M6}$), which depends upon I_B, generates a current flowing through R_2 (I_{R2}) that can be expressed as

$$I_{R2} = \frac{V_{GS,M6}(I_B)}{R_2}. \quad (5)$$

From [15, 16] and Eq. (5), I_{R2} is considered to be a CTAT current because $V_{GS,M6}$ decreases with increasing temperature at any fixed drain current.

The sum of the two currents generated by the PTAT current generator and the CTAT current generator flows through a resistor R_3 and generates V_{REF}, which can be derived from Eqs. (4, 5) as

$$V_{REF} = R_3\left\{\frac{K_{M10}}{K_{M3}} \cdot \frac{\eta kT \ln(K_{M2}/K_{M1})}{qR_1} + \frac{K_{M9}}{K_{M8}} \cdot \frac{V_{GS,M6}(I_B)}{R_2}\right\}. \quad (6)$$

3. Current-to-frequency Converter

Fig. 4 shows a schematic of the current-to-frequency converter with the PTAT current generator, which consists of the integrator and the hysteresis comparator, and converts I_{PTAT} to f_{PTAT}. In a previous work [11], when

a drain current of a transistor used as a current source flows through the capacitor between the ground and the drain of a transistor, the drain voltage causes variations in the voltage between the drain and source of a transistor. The above voltage variation brings about a drain current variation, which results in error in the sensing operation when the voltage margin is insufficient at a low supply voltage. To solve this problem, an integrator is employed to maintain the voltage between the source and drain of M_{PTAT} ($V_{DS,MPTAT}$) and thus to make I_{PTAT} constant during the integration operation. V_{CMP} generated by integrating I_{PTAT} can be expressed as

$$V_{CMP} = -\frac{1}{C_F}\int I_{PTAT}\,dt, \tag{7}$$

where C_F is the feedback capacitance. V_{CMP} is compared with V_{REF} from the reference voltage generator and VSS in the hysteresis comparator. The output of the hysteresis comparator is high when V_{CMP} is greater than V_{REF}, and low when V_{CMP} is less than VSS. The hysteresis comparator holds its previous value when V_{CMP} is greater than VSS and less than V_{REF}. From Eqs. (3, 7), f_{PTAT} can be expressed as

$$f_{PTAT} = \frac{K_{MPTAT}}{K_3}\cdot\frac{\eta kT\ln\left(K_{M2}/K_{M1}\right)C_{SC}f_{REF}}{qV_{REF}C_F}. \tag{8}$$

Therefore, f_{PTAT} is linearly proportional to temperature and fed to reset the input and output of the integrator to V_{REF}.

IV. Measurement Results

Fig. 5 shows a photomicrograph of the proposed temperature sensor that was fabricated using a 90 nm CMOS process. The temperature sensor occupies an active area of 1300 × 530 μm^2 and consumes an energy of 36 pJ per conversion. Ten sample chips were measured in a temperature chamber over the temperature range of 0 to 70°C, at intervals of 10°C.

Fig. 6 shows the measurement results of f_{PTAT} with respect to temperature, ranging from 69.26 to 98.17 kHz, representing that f_{PTAT} varies linearly with temperature, with an average temperature coefficient of 218 Hz/°C. Fig. 7 shows that the measured temperature error ranges

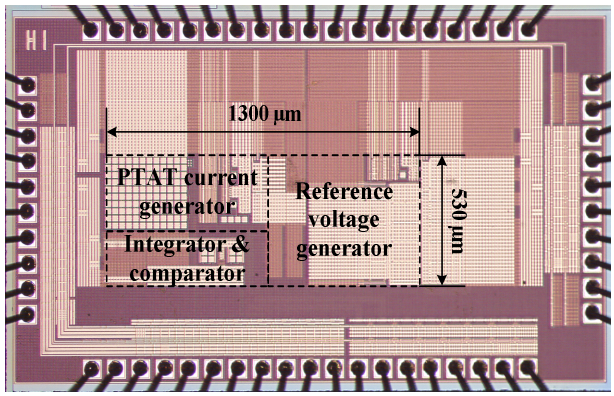

Fig. 5. Photomicrograph of the fabricated chip.

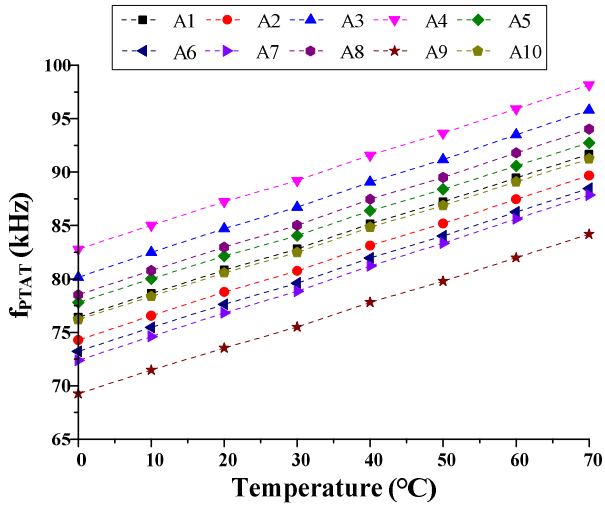

Fig. 6. Measurement results of PTAT frequency (f_{PTAT}) with respect to temperature.

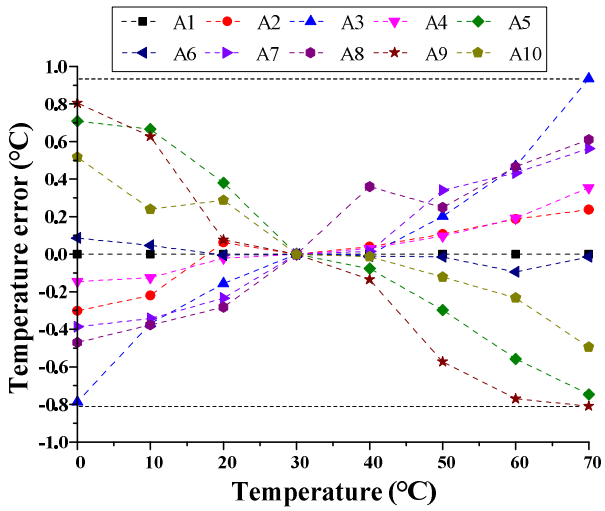

Fig. 7. Measurement results of the temperature error with respect to temperature.

Table 1. Performance comparison

Parameter	This work	[6]	[7]	[8]	[9]	[10]
Process (μm)	0.09	0.35	0.18	0.18	0.18	0.18
Sensor Type	Frequency	Delay	Duty cycle	Frequency	Frequency	Delay
Temperature Range (°C)	0 to 70	−40 to 80	−30 to 70	−30 to 60	−20 to 30	−30 to 70
Temperature error (°C)	−0.81 to +0.94	±1	±1.3	±1.5	±0.8	−0.7 to +0.6
Supply voltage (V)	1.2	3	1.8	1	1	1
Power consumption (μW)	2.2	9	7.2	0.35	2.4	0.092
Energy/Conversion (J/Conversion)	36p	0.45μ	—	5.1n	96n	92p
Area (mm^2)	0.689	0.4	0.34	0.14	1.1	0.021
Calibration	1-point	2-point	1-point	1-point	1-point	1-point

from −0.81 to +0.94°C after one-point calibration at 30°C.

Table 1 compares the performance of the proposed temperature sensor to that of prior temperature sensors. The proposed temperature sensor consumes the least energy per conversion among the sensors compared.

V. CONCLUSIONS

We propose a temperature sensor based upon subthreshold MOSFETs for low-voltage and low-power on-chip thermal monitoring applications. To improve the temperature accuracy of the proposed temperature sensor, an error amplifier and an integrator are used to minimize the error of the PTAT currents and to maintain constant PTAT current during the integrating operation, respectively. The proposed temperature sensor was fabricated using a 90 nm CMOS process with a supply voltage of 1.2 V. The measured temperature error of the fabricated sensors ranges from −0.81 to +0.94°C in the temperature range of 0 to 70°C after one-point calibration at 30°C. In addition, the proposed temperature sensor consumes an energy of 36 pJ per conversion, the lowest energy consumption compared with prior works. Therefore, the proposed temperature sensor is suitable for low-voltage and low-power on-chip thermal monitoring applications.

ACKNOWLEDGMENTS

This work was supported by the National Research Council of Science & Technology (NST) grant by the Korea government (MSIP) (No. CMP-16-05-ETRI).

REFERENCES

[1] J. Long, S. O. Memik, G. Memik, and R. Mukherjee, “Thermal monitoring mechanisms for chip multiprocessors,” *ACM Trans. Archit. Code Optim.*, vol. 5, no. 2, pp. 1–33, Aug. 2008.

[2] C.-C. Chung and C.-R. Yang, “An autocalibrated all-digital temperature sensor for on-chip thermal monitoring,” *IEEE Trans. Circuits Syst. II, Exp. Briefs*, vol. 58, no. 2, pp. 105–109, Feb. 2011.

[3] H. Lakdawala, Y. W. Li, A. Raychowdhury, G. Taylor, and K. Soumyanath, “A 1.05 V 1.6 mW, 0.45°C 3σ resolution ΣΔ based temperature sensor with parasitic resistance compensation in 32 nm digital CMOS process,” *IEEE J. Solid-State Circuits*, vol. 44, no. 12, pp. 3621–3630, Dec. 2009.

[4] M. Sasaki, M. Ikeda, and K. Asada, “A temperature sensor with an inaccuracy of −1/+0.8 °C using 90-nm 1-V CMOS for online thermal monitoring of VLSI circuits,” *IEEE Trans. Semicond. Manuf.*, vol. 21, no. 2, pp. 201–208, May 2008.

[5] L. Lu, S. Block, D. E. Duarte, and C. Li, “A 0.45-V MOSFETs-based temperature sensor front-end in 90 nm CMOS with a noncalibrated ±3.5°C 3σ relative inaccuracy from −55°C to 105°C,” *IEEE Trans. Circuits Syst. II, Exp. Briefs*, vol. 60, no. 11, pp. 771–775, Nov. 2013.

[6] P. Chen, T.-K. Chen, Y.-S. Wang, and C.-C. Chen, “A time-domain sub-micro Watt temperature sensor with digital set-point programing,” *IEEE Sens. J.*, vol. 9, no. 12, pp. 1639–1646, Dec. 2009.

[7] S. S. Chouhan and K. Halonen, “Design and implementation of micro-power temperature to duty cycle converter using differential temperature

sensing," *Microelectronics J.*, vol. 46, no. 6, pp. 482–489, June 2015.

[8] B. Wang, M.-K. Law, A. Bermak, and H. C. Luong, "A passive RFID tag embedded temperature sensor with improved process spreads immunity for a −30°C to 60°C sensing range," *IEEE Trans. Circuits Syst. I, Reg. Papers*, vol. 61, no. 2, pp. 337–346, Feb. 2014.

[9] J. Yin et al., "A system-on-chip EPC Gen-2 passive UHF RFID tag with embedded temperature sensor," *IEEE J. Solid-State Circuits*, vol. 45, no. 11, pp. 2404–2420, Nov. 2010.

[10] F. Deng, Y. He, B. Li, L. Zhang, X. Wu, Z. Fu, and L. Zuo, "Design of an embedded CMOS temperature sensor for passive RFID tag chips," *Sensors*, vol. 15, no. 5, pp. 11442–11453, May 2015.

[11] V. Szekely, C. Marta, Z. Kohari, and M. Rencz, "CMOS sensors for on-line thermal monitoring of VLSI circuits," *IEEE Trans. Very Large Scale Integr. (VLSI) Syst.*, vol. 5, no. 3, pp. 270–276, Sep. 1997.

[12] G. Nenna, *et al*., "A study on thermal degradation of organic LEDs using IR imaging," *Macromol. Symp.*, vol. 247, no. 1, pp. 326–332, Feb. 2007.

[13] B. Razavi, *Design of Analog CMOS Integrated Circuits*. Boston, MA, USA: McGraw-Hill, 2001.

[14] A. Wang, B. H. Calhoun, and A. P. Chandrakasan, *Sub-threshold Design for Ultra Low-Power Systems*. New York, NY, USA: Springer-Verlag, 2006.

[15] G. Giustolisi, G. Palumbo, M. Criscione, and F. Cutri, "A low-voltage low-power voltage reference based on subthreshold MOSFETs," *IEEE J. Solid-State Circuits*, vol. 38, no. 1, pp. 151–154, Jan. 2003.

[16] X. Cai, L. Luo, and Z. Li. "The design of sub-threshold reference circuit using resistor temperature compensation," in *Proc. IEEE Int. Midwest Symp. Circuits Syst.*, pp. 78–81, Aug. 2009.

Jun-Seok Na received a B.S. degree in electronics and computer engineering from Hanyang University, Seoul, Korea, in 2010. He is currently pursuing a Ph.D. degree in electronics and computer engineering at Hanyang University. His research interests include driving circuits for microdisplay applications and readout circuits for sensor applications.

Woosul Shin received a B.S. degree in electrical engineering from Hanyang University, Seoul, Korea, in 2014. He is currently pursuing an M.S. degree in electronics and computer engineering at Hanyang University. His interests include active matrix flat panel displays and display driver ICs.

Bong-Choon Kwak received B.S. and M.S. degrees in electronics and computer engineering from Hanyang University, Seoul, Korea, in 2010 and 2012, respectively, and is currently pursuing a Ph.D. degree in electronics engineering at Hanyang University. His research interests include driving circuits for microdisplay applications.

Seong-Kwan Hong received a Ph. D. degree in electrical engineering from Georgia Institute of Technology, Atlanta, GA, USA, in 1994. He is currently a Research Professor at Hanyang University, Seoul, Korea.

Oh-Kyong Kwon received a Ph. D. degree in electrical engineering from Stanford University, Stanford, CA, USA, in 1988. He is currently a Professor with the Department of Electronic Engineering, Hanyang University, Seoul, Korea.